Initial FAST observations of acceleration processes in the cusp

R. Pfaff[1], J. Clemmons[1,2], C. Carlson[3], R. Ergun[3], J. McFadden[3], F. Mozer[3],
M. Temerin[3], D. Klumpar[4], W. Peterson[4], E. Shelley[4], E. Mœbius[5],
L. Kistler[5], R. Strangeway[6], R. Elphic[7], C. Cattell[8]

Abstract. FAST satellite observations during two encounters with the Earth's cusps near 4000 km are presented. In addition to precipitating magnetosheath particles with isotropic pitch angle distributions, the energetic particle data reveal upgoing ion beams, ion conics, downgoing "inverted-V" electron distributions, and very narrow, intense upgoing electron beams. A rich assortment of DC-coupled electric fields and plasma waves accompany these acceleration processes. In one example, step-like injections of magnetosheath ions are correlated with bursts of upgoing ion beams and downgoing electrons, suggesting that the currents associated with these injections set up local electric potential structures that subsequently drive the acceleration processes. The observations underscore the fact that the cusp is not merely a conduit for the passage of magnetosheath particles and fields, but contains a dynamic internal electrical structure that accelerates particles locally and may alter the precipitating magnetosheath particle populations themselves.

Introduction and Data Presentation

Although the Earth's cusps provide conduits through which waves and energetic particles pass between the magnetosheath and upper atmosphere, they also represent regions within which charged particles may be energized by local acceleration processes. To study these complex relations, we have examined in detail about 35 encounters of the FAST satellite with the cusp regions. Evidence for local acceleration is a common feature of these passes, as described here using two representative data sets. An overview of the FAST satellite including its instruments and their operation is presented in Carlson et al. [this issue (a)].

The FAST data shown here were gathered on two passes near magnetic noon at ~4000 km in the winter northern hemisphere. For both events, although the satellite was in sunlight, the ionosphere below its location was in darkness. Coincident with both sets of observations, the interplanetary magnetic field was oriented southward, as determined by the Wind satellite magnetometer [Lepping, personal communication, 1997].

Survey Data. Survey data for two cusp encounters are shown in Figure 1(a,b). The cusp region is identified by the intense wave emissions and particle fluxes that comprise the central ~2.5 minutes of data which represent ~600 km of horizontal distance.

[1]NASA/Goddard Space Flight Center, Greenbelt, MD
[2]Now at: Aerospace Corporation, El Segundo, CA
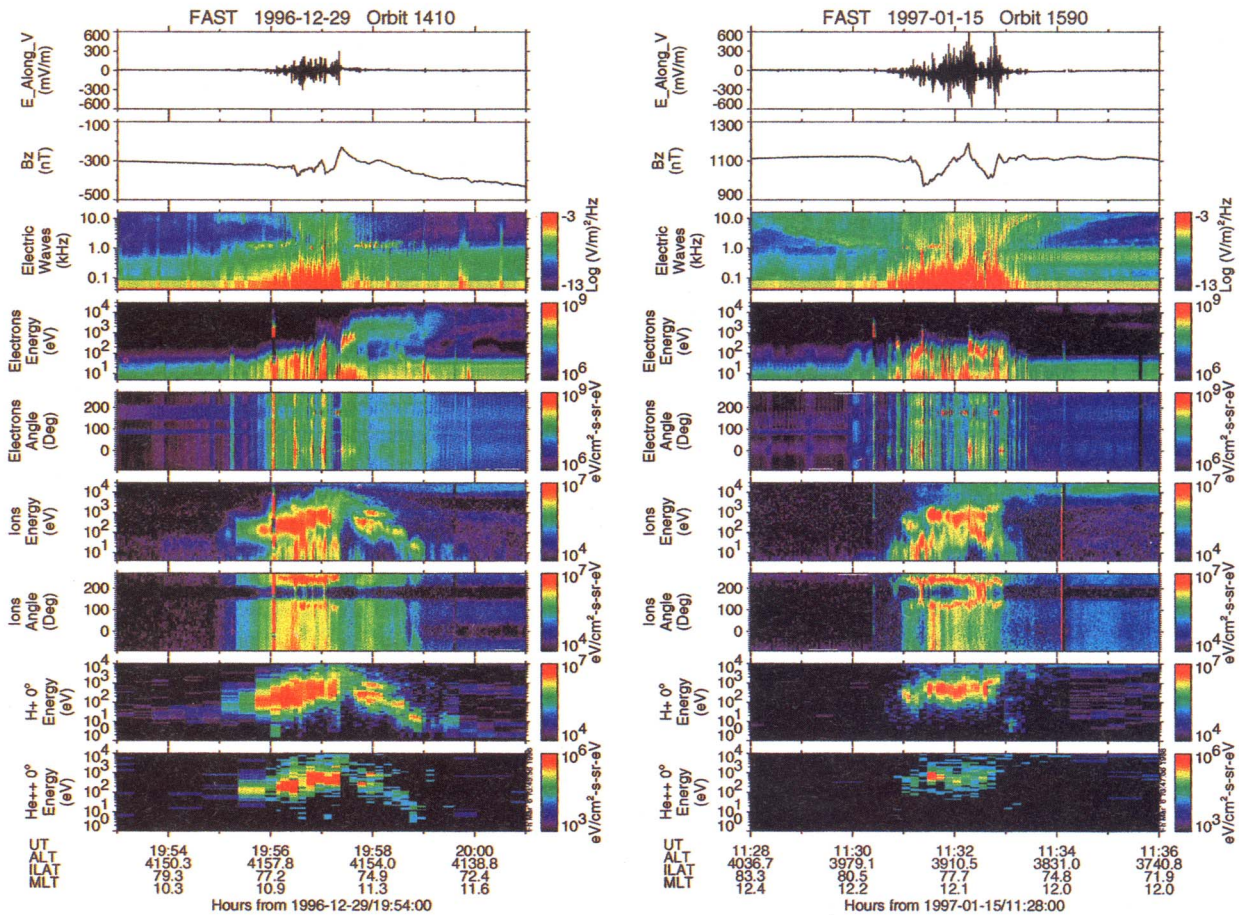[3]Space Sciences Laboratory, Univ. of California, Berkeley, CA
[4]Lockheed Palo Alto Laboratory, Palo Alto, CA
[5]University of New Hampshire, Durham, NH
[6]IGPP, Univ. of California, Los Angeles, CA
[7]Los Alamos National Laboratory, Los Alamos, NM
[8]School of Physics and Astronomy, Univ. of Minn., Minneapolis, MN

The top three panels of Figure 1(a,b) display the fields data. For each pass, the upper panel shows DC-coupled electric fields along the direction of the satellite velocity, sampled at 512 s^{-1} (in the central portion of the figure). Notice the intense electric field excursions that often exceed ± 200 mV/m. The second panel shows the spin-axis component of the DC magnetometer oriented perpendicular to the orbital plane. Its large variations provide evidence for zonally-oriented sheets of field-aligned currents. The third panel is a 0.04-16 kHz wave spectrogram detected along one electric field spin plane component. The data show localized plasma waves in the cusp region with the most intense amplitudes at the lowest frequencies (< ~500 Hz). At higher frequencies, V-shaped emissions are present which we associate with electromagnetic auroral hiss. Narrow emissions at the lower hybrid frequency near 1 kHz can also be discerned here. A band of ELF hiss extends equatorward of the cusp in Figure 1(b).

The energetic electron and ion fluxes are shown next, grouped in two pairs of panels. The first panel of each pair consists of an energy-time spectrogram from 5 eV to 30 keV for all pitch angles while the second panel shows pitch angle data for all such energies, from $-90°$ to $270°$. (Note: although pitch angles only exist between $0°$ and $180°$, here we combine two hemispherical detectors to obtain $360°$ measurements.) For these northern hemisphere observations, $0°$ corresponds to downgoing, field-aligned particles and $180°$ corresponds to upgoing, anti-field-aligned particles. Both the electron and ion spectrograms show localized, intense particle fluxes in the cusp regions coincident with the enhanced plasma waves, DC-coupled electric fields, and magnetometer current signatures. Notice the electron spectra include bursts of narrow energy spectra with peaks at a few hundred eV as well as strong electron bursts at lower energies.

The energetic ions include fluxes that extend to higher energies than the electrons. The dominant cusp ions typically include broad spectra with energies between 0.1 and 2 keV and which frequently appear continuous in time within the cusp, at least on compressed time scales. In Figure 1(a), the ion energy reveals a typical dispersion with time, shifting to higher energies as the satellite approaches the equatorward cusp boundary [e.g., Reiff et al., 1977]. These ions have pitch angle distributions that are isotropic (except for the loss cone) and we associate them with precipitating particles that originate at the magnetosheath. The ion spectrograms also show bursts of intense fluxes at lower energies that appear along with the magnetosheath ions. As shown in detail below, these lower energy ions correspond to the upgoing ion beams and ion conics, both of which are associated with local acceleration mechanisms. A weaker ion component at the highest energies (> 10 keV) is observed in, and equatorward of, the cusp and is presumably of plasma sheet origin.

The lower two panels of Figure 1(a,b) from the time-of-flight energy and mass spectrometer, provide a measure of the ion fluxes corresponding to H$^+$ and He^{++}, integrated for pitch angles between ±45°. These panels reveal significant populations of downgoing ions from about 0.1 keV to several keV that are composed mainly of protons that we interpret as originating at the

Figure 1. Survey FAST data for two cusp encounters. U.T. times are HR:MIN. See text for details.

magnetosheath. Notice that there are effectively no lower energy downgoing H^+ ions associated with either of the two cusp passes. The data also reveal the presence of He^{++} ions as part of this population. This result reinforces our identification of the cusp since He^{++} ions are known to enter the cusp via the magnetosheath [Shelley et al., 1976] and do not otherwise exist in appreciable quantities in the ionosphere or lower magnetosphere.

High Resolution Observations. High resolution data within each cusp encounter gathered as bursts triggered by the FAST on-board computer are shown in Figure 2(a,b). Each burst is ~16s and the data shown here correspond to five nearly contiguous bursts. (Gaps between bursts are indicated by white areas.)

The particle data shown in the lower four panels in Figure 2(a,b) correspond to the same such panels in Figure 1(a,b). Bursts of both upgoing and downgoing electrons are shown in the upper two of these panels. The downgoing electron spectra peak near a hundred eV with comparatively narrow spectral widths and relatively broad pitch angle distributions centered at 0°. The upgoing electrons, on the other hand, have broader energy spectra from a few to a few hundred eV but their pitch angles are very narrow and are centered at 180°. These upgoing electrons constitute the most intense electron fluxes observed in these cusp passes. Notice that the groupings of upgoing electrons sometimes consist of a series of very short bursts of narrow upgoing electron beams, particularly near 11:31:50 U.T. in Figure 2(b).

The energetic ions basically show two populations: the downgoing ~ keV ions associated with the sheath precipitation discussed earlier, and lower energy (few hundred eV) ions that

appear as ion conics and as upgoing ion beams. The ion beams are characterized by a peak in the energy spectra at several tens of eV coincident with a narrowed pitch angle spread which is directed up along the magnetic field line at 180° (see, for example, the ion beams at 19:57:03 U.T. in Figure 2(a) and the beam at 11:32:28 U.T. in Figure 2(b)). Notice that the upgoing ion beams often appear simultaneously with bursts of downgoing electrons (particularly in Figure 2(a)), consistent with their acceleration by an upwards-directed electric field parallel to the magnetic field. The ion conics exist between the upgoing ion beams and are characterized by their narrow symmetric pitch angles centered near 120° and 240°. Notice further that the ion beams and conics "interleave" in the spacecraft frame with the upgoing electron beams (particularly in Figure 2(b)). In other words, the narrow beams of upgoing electrons are shut off during times when upgoing ions are observed and vice-versa, implying reversals of the parallel electric field. For the data in Figure 2(a), notice further that the precipitating magnetosheath ions appear to "step" in energy between 19:56:25 and 19:57:05 and that this modulation corresponds to that of the bursts of intense downward electron fluxes and upwards ion beams.

The particle fluxes create currents which are apparent in the zonal magnetometer component shown in the panel just above the particle data in Figure 2(a,b). Notice that for downgoing currents (upgoing electron beams), the magnetometer signal provides a positive slope, while the opposite is true for upgoing currents (downgoing electrons). This correlation extends to the smallest observable features in the magnetometer trace and has been
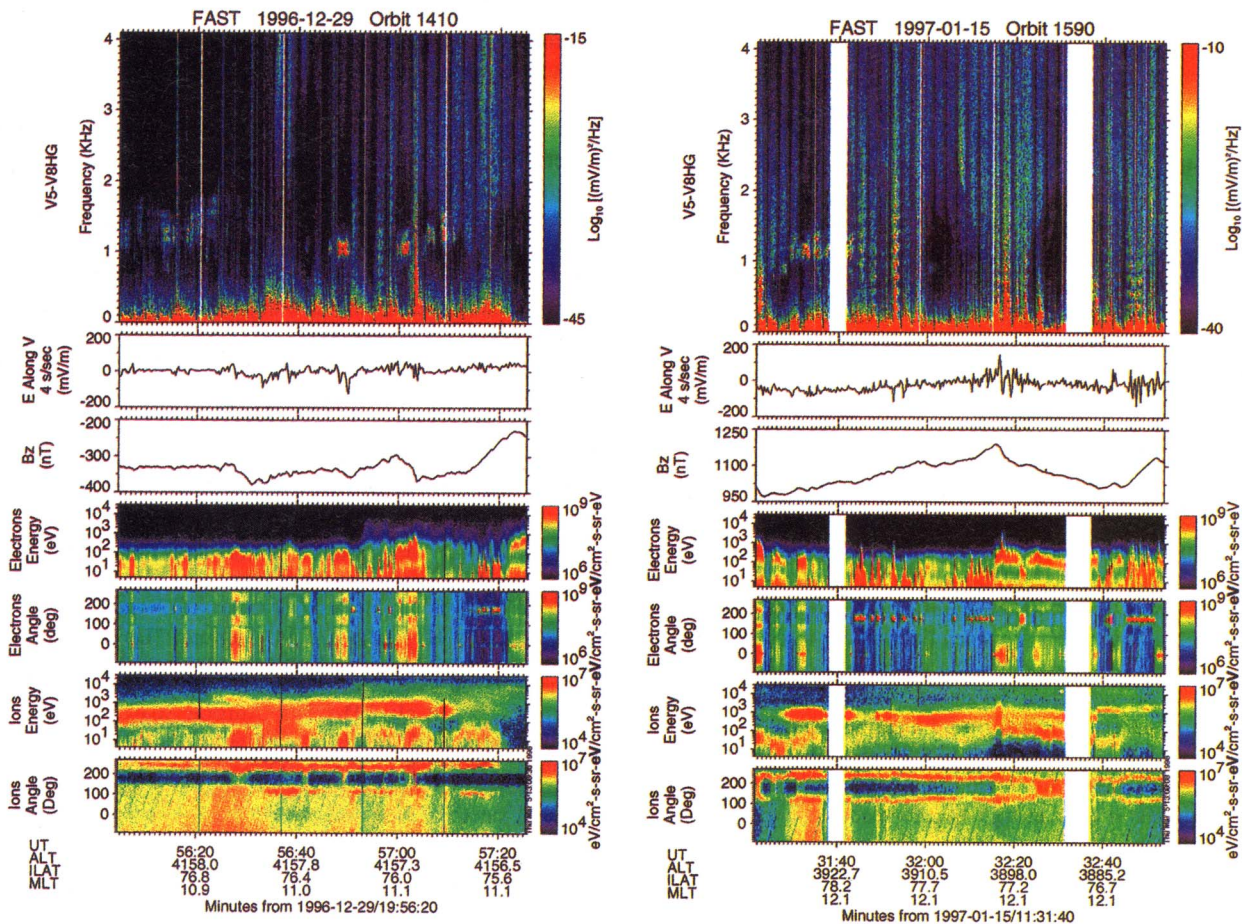
Figure 2. Particle and fields data for expanded time intervals for the observations shown in Figure 1. U.T. times are MIN:SEC. The faint diagonal stripes in the lowest panel are due to a slight blockage of the ion detector by the electric field boom.

discussed for auroral zone FAST observations by Elphic et al. [this issue]. Such a correlation using this single component is consistent with magnetic field deviations that are due to zonally-oriented sheets of field-aligned currents.

Finally, the electric field data associated with the energetic particles are shown in the upper two panels of Figure 2(a,b). The uppermost panel is a 0-4kHz spectrogram of the DC-coupled electric field data corresponding to a spin plane component and the panel beneath this shows the DC electric field data along the spacecraft velocity vector at 4 s^{-1}. The spectral wave data show a strong twice-per spin (2.5s) modulation which occurs as the electric field double probe rotates through the perpendicular and parallel directions with respect to the magnetic field. Notice that the waves are not uniform within the cusp region, but exhibit enhancements that correlate with bursts of large amplitude DC-coupled electric fields as well as accelerated particles.

Intense low frequency waves characterize the entire cusp encounter and extend to several hundred Hz [e.g., Gurnett and Frank, 1978]. The wave spectrograms show emissions separated by the proton cyclotron frequency, Ω_{H^+}, of ~ 200 Hz which we generally associate with Bernstein mode and ion-ion mode emissions. The spectrograms also show emissions at the lower hybrid frequency near 1.1 kHz with small bifurcations in frequency. Higher frequency (>1 kHz) electromagnetic emissions appear associated with upgoing electron bursts.

Discussion and Summary

The FAST observations reveal a rich interplay of enhanced energetic particle fluxes and electric fields. The data show that the magnetospheric cusp near 4000 km supports three general plasma populations: (1) that which originates at the magnetosheath and does not undergo further acceleration; (2) magnetosheath plasma that undergoes local acceleration much nearer to the Earth; and (3) accelerated ionospheric plasma which constitute the upgoing particle beams.

The measurements of narrow upgoing ion and electron beams as well as the downgoing electron fluxes and ion conics not only show that acceleration processes occur on relatively short time and distance scales in the cusp, but also that such processes must include mechanisms operating both above and below the spacecraft altitude of 4000 km. In fact, the absence of downgoing ion beams associated with the narrow, upgoing electron beams suggests that those beams are accelerated below the spacecraft. Furthermore, the ion beams, conics, and accelerated electron fluxes appear remarkably similar to the same such phenomena routinely observed in the nightside auroral zone, including the extremely narrow, upgoing electron beams that constitute very intense fluxes with a broad low energy spectrum [Carlson et al., this issue, (b)] and the patterns of ion conics whose pitch angles and energies smoothly taper to form upgoing ion beams [McFadden et al., this issue].

The downward-directed electrons observed by the FAST particle detectors in the cusp are similar to the inverted-V distributions that are usually associated with the aurora, although at reduced peak energies. These narrow electron spectra peak at a few hundred eV instead of keV energies that are typically associated with visible arcs in the auroral zone and are likely the same phenomena energized at lower levels. The downgoing, peaked electron spectra appear in small bursts rather than the more-or-less continuous streams of precipitating electrons that are injected at the magnetosheath. Furthermore, the FAST observations show that the downgoing electrons are switched off when the upgoing electron beams are detected, indicating that the polarity of the accelerating fields has switched. This observation underscores the fact that these downgoing electron fluxes are accelerated on short time and distance scales in the cusp, presumably by a local mechanism, and are distinct from the unaccelerated magnetosheath electrons. The downgoing electron fluxes observed by FAST are similar to accelerated electrons previously reported in the cusp by instruments on other spacecraft [e.g., Lin et al., 1986; Woch and Lundin, 1992], whereas the narrow, upgoing electron fluxes in the cusp resemble those reported by Burch et al. [1983].

An important aspect of the observations reported here is the correlation in Figure 2(a) between the steps or discontinuities in energy spectra of the precipitating magnetosheath ions with the appearance of individual bursts of well-defined acceleration phenomena, such as the downward electron bursts and upgoing ion beams observed between 19:56:25 and 19:57:05 in Figure 2(a). Magnetosheath ions in the cusp often display sharp discontinuities in their energy spectra associated with transient features such as pulsed reconnection or solar wind pressure pulses [e.g., Smith and Lockwood, 1996]. This correlation implies that the energy source for the acceleration processes is provided by the currents associated with the precipitating magnetosheath particles and suggests that such injections enable enhanced electric fields, such as those associated with the beams in Figure 2(a), to be set up at lower altitudes within the cusp. Parallel potential drops that accompany such fields would then create the upgoing ion beams and downward, inverted-V electron fluxes.

Precipitating magnetosheath ion populations may also be influenced by such local acceleration processes, as discussed by Torbert and Carlson [1980]. In this case, we would expect the fluxes of the magnetosheath ions to be diminished in the presence of upgoing ion beams due to the presumed upward-directed electric fields associated with them. No such correlations are readily apparent in these two examples. It is particularly difficult to establish such correlations because the magnetosheath ions are modulated in space and time at their source. For example, at 11:31:45 in Figure 2(b), the magnetosheath ion fluxes are strongly diminished, although there is no appearance of an upgoing ion beam, or change in the electron spectra, that would indicate that this magnetosheath ion variation was due to that of the local potentials. On the other hand, the abrupt discontinuity in the magnetosheath ion spectrum at 11:32:38.5 in Figure 2(b), does correspond to a shutting off of downgoing, accelerated electrons, and suggests a relation between the acceleration process and the magnetosheath ion discontinuity.

The most plausible mechanism to create the observed narrow electron and ion beams in the cusp region is that of parallel potential drops, as have been postulated to explain similar phenomena in the auroral zone [e.g., Mozer et al., 1980]. The FAST electric field data presented here reveal evidence for electrostatic spatial structures associated with many of the electron and ion beams within these cusp crossings, which may be associated with parallel electric fields. Indeed, Lin et al. [1986] using simultaneous DE-1 and DE-2 satellite observations

of energetic electrons at two altitudes in the cusp concluded that some parallel potential must account for the enhanced energy flux observed in the lower altitude electrons.

Summary. The observations gathered by the FAST satellite indicate that local acceleration processes similar to those in the auroral zone also occur in the cusp, and show further evidence that the cusp is not merely a passive conduit for the passage of magnetosheath particles and fields to the upper atmosphere. Furthermore, the data shown here suggest that currents and fields associated with magnetosheath particle injections supply the energy source to create such acceleration processes, since one example of step-like magnetosheath ions appears to correlate with bursts of locally accelerated upward ion beams and downward electron fluxes. This situation is analogous to interactions between the plasma sheet particles and the ionosphere where similar potential structures are set up to create the visible aurora. Such acceleration processes appear widespread in nature and are likely to occur in magnetically-coupled interface regions between hot, injected magnetospheric plasma and the cool ionosphere.

References

Burch, J. L., P. H. Reiff, and M. Sugiura, "Upward electron beams measured by DE-1: a primary source of dayside region-1 Birkeland currents," *Geophys. Res. Lett.*, 10, 753, 1983.

Carlson, C. W., et al., "The Fast Auroral Snapshot mission," *Geophys. Res. Lett.*, this issue, 1998a.

Carlson, C. W., et al., "FAST observations in the downward auroral current region: Energetic up-going electron beams, parallel electric fields, and ion heating," *Geophys. Res. Lett.*, this issue, 1998b.

Elphic, R. C., et al., "The auroral current circuit and field-aligned currents observed by FAST," *Geophys. Res. Lett.*, this issue, 1998.

Gurnett, D. A., and L. A. Frank "Plasma waves in the polar cusp: observations from Hawkeye 1," *J. Geophys. Res.*, 83, 1447, 1978.

Lin, C., et al., "Near-conjugate observ. of polar cusp electron precipitation using DE 1 and DE 2," *J. Geophys. Res.*, 91, 11186, 1986.

McFadden, J. P., et al., "Spatial structure and gradients of ion beams observed by FAST," *Geophys. Res. Lett.*, this issue, 1998.

Mozer, F. S., et al., "Satellite measurements and theories of low altitude auroral particle acceleration," *Space. Sci. Rev.*, 27, 155, 1980.

Reiff, P. H., T. W. Hill, J. L. Burch, "Solar wind plasma injection at the dayside magnetospheric cusp," *J. Geophys. Res.*, 82, 479, 1977.

Shelley, E. G. et al., "He^{++} and H^{+} flux measurements in the dayside magnetospheric cusp," *J. Geophys. Res.*, 81, 2363, 1976.

Smith, M. F., and M. Lockwood, "Earth's magnetospheric cusps," *Rev. Geophys.*, 34, 233, 1996.

Torbert, R., and C. Carlson, "Evidence for parallel electric field particle acceler. in the dayside auroral oval," *J. Geophys. Res.*, 85, 2909, 1980.

Woch, J. and R. Lundin, "Magnetosheath plasma precipitation in the polar cusp and its control by the IMF," *J. Geophys. Res.*, 97, 1421, 1992

C. Carlson, R. Ergun, J. McFadden, F. Mozer, M. Temerin, Space Sciences Laboratory, Univ. of California, Berkeley, CA

C. Cattell, School of Physics and Astronomy, Univ. of Minnesota, MN

J. Clemmons, Aerospace Corp., El Segundo, CA

R. Elphic, Los Alamos National Laboratory, Los Alamos, NM

D. Klumpar, W. Peterson, E. Shelley, Lockheed PAL, Palo Alto, CA

L. Kistler, E. Mœbius Univ. of New Hampshire, Durham, NH

R. Pfaff, NASA/Goddard Space Flight Center, Greenbelt, MD, 20771

R. Strangeway, IGPP, Univ. of California, Los Angeles, CA